

Phonon Softening in Superconducting Diamond

M. Hoesch,¹ T. Fukuda,¹ T. Takenouchi,² J.P. Sutter,³ S. Tsutsui,³
A.Q.R. Baron,³ M. Nagao,⁴ Y. Takano,⁴ H. Kawarada,² and J. Mizuki¹

¹*SPring-8, JAEA, 1-1-1 Kouto, Sayo, Hyogo, Japan*

²*School of Science and Engineering, Waseda University, 3-4-1 Okubo, Shinjuku, Tokyo, Japan*

³*SPring-8, JASRI, 1-1-1 Kouto, Sayo, Hyogo, Japan*

⁴*National Institute for Materials Science, 1-2-1 Sengen, Tsukuba, Japan*

(Dated: May 24, 2019)

Phonons in a highly boron-doped CVD grown epitaxial diamond layer have been measured by inelastic x-ray scattering. The sample shows a superconducting transition at $T_c = 4.2$ K. The optical modes are strongly softened up to 7 meV close to the Brillouin zone centre and 2 meV at the zone boundary while acoustic modes do not soften. This observation confirms the strong electron-phonon coupling in superconducting diamond and the momentum dependence is consistent with the presence of a spheroid Fermi surface that gives rise to strong softening for phonon momenta smaller than the maximal spanning vectors.

When superconductivity in heavily boron-doped diamond was discovered [1], two main questions had to be addressed to understand this phenomenon. (i) The nature of the charge carriers had to be established and (ii) the coupling mechanism that leads to the formation of Cooper pairs needed to be investigated. The discovery of superconductivity was soon confirmed by other groups in samples grown by chemical vapour deposition (CVD) [2, 3] and type II bulk superconductivity was clearly established by a number of experimental observations [4]. Boron is found to occupy substitutional sites in the slightly expanded diamond lattice and the colour changes to dark grey. In this paper we address the question of the coupling mechanism through the study of the lattice dynamics of heavily B-doped diamond by inelastic x-ray scattering (IXS) experiments. The doping levels of a few atomic percent, where superconductivity has been observed, are well above the metal-to-insulator transition (MIT) at $3 \cdot 10^{20} \text{ cm}^{-3}$ [5], but they lead to a metallic state with a rather low carrier concentration. A strong coupling mechanism must be present to give rise to the quite substantial transition temperatures of up to $T_c = 11$ K (onset of superconductivity [6]).

Diamond is well known for its extreme hardness due to the short covalent bonds. The two atomic basis leads to six phonon branches, with a steep dispersion of the acoustic modes and a very high frequency of the optical modes. The lattice dynamics of undoped diamond have been investigated experimentally for a long time [7] and minute details such as the over-bending of the longitudinal optical (LO) branch have been studied both by inelastic neutron and x-ray scattering techniques [8].

The electronic structure of undoped diamond features a large indirect band gap of 5.5 eV. The top of the valence band around the Γ -point consists of three branches of carbon sp -electrons that form the two pockets of light and heavy holes. Light doping of diamond with boron leads to an acceptor level with a binding energy of 0.37 eV and semiconducting conductivity [9].

The nature of the metallic state above the MIT is determined by the hybridization of the impurity states between neighbouring B sites and with the C sp -band. The overlap of impurity states alone could lead to a metallic impurity band above the valence band maximum. In the other extreme of strong hybridization with the carbon host a metallic band is formed in the top region of the diamond valence band. The latter scenario is the basis for several theoretical studies that rely on *ab initio* calculations in the virtual crystal approximation (VCA) [10, 11, 12]. It is supported by supercell calculations [13, 14, 15] and by angle resolved photoemission experiments [16]. Evidence for the persistence of a metallic impurity band (the first scenario) was on the other hand provided by optical spectroscopy [17]. A mixture between both scenarios is possible. In either case the effects of disorder due to the high density of impurity atoms need to be considered in a complete picture of the electronic structure [15]. The local lattice distortion around impurity atoms and the possibility of interstitial site occupation of impurity atoms also need to be taken into account.

The coupling mechanism that leads to superconductivity can be provided by electron-phonon coupling. Evidence for a strong electron-phonon coupling was found by Raman scattering spectroscopy. In pure diamond the zone centre optical mode appears as a strong single peak at 1330 cm^{-1} (164 meV). At high B doping levels a broad second peak appears at 1230 cm^{-1} with a Fano-like lineshape [18]. The single phonon peak is shifted to lower frequencies with increased doping and decreases in intensity. In our superconducting sample the single phonon peak becomes hardly discernible in the broad intensity of the second feature. A shift of $25 - 35 \text{ cm}^{-1}$ (3.7 ± 0.7 meV) was determined by a peak fitting procedure. The existence of a Fano feature gives evidence for the coupling of the phonons to a continuum of electronic states and the shift of the one phonon peak reflects the phonon softening, but a quantitative analysis of the

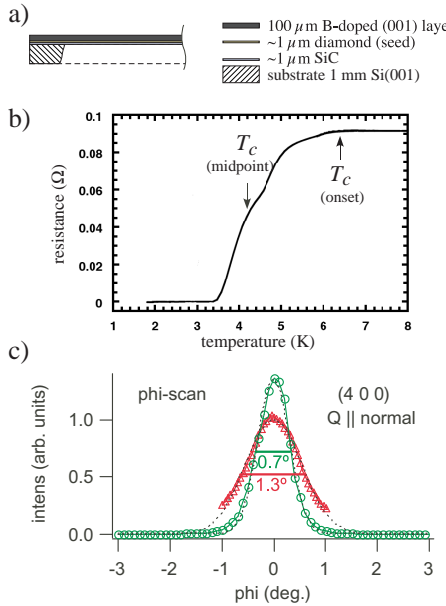


FIG. 1: (a) Schematic view of the $\approx 100\mu\text{m}$ thick B-doped sample B. (b) Temperature-dependent resistance curve. Above T_c the resistance is almost flat with a room temperature resistivity of $\approx 15\ \Omega\text{cm}$. (c) X-ray rocking curves of the (004) reflection of sample B (\circ) and N-doped sample N (Δ).

electron-phonon coupling strength is not possible from the Raman data [18].

Epitaxially grown B-doped diamond was prepared by microwave plasma assisted CVD growth (sample B) [19]. The B-doped material was deposited on an existing $1\mu\text{m}$ thick heteroepitaxially grown N-doped diamond film on $1\mu\text{m}$ SiC on Si(001). A total film thickness of $\approx 100\mu\text{m}$ was achieved by 106 hrs. of CVD growth in 10 sessions à 5 - 20 hrs. each. The B-content in the film was $3.8 \cdot 10^{21}\text{cm}^{-3}$ (2.5 at%). The superconducting transition begins at $T_c = 6.4\ \text{K}$ with a midpoint at 4.2 K as shown in Fig. 1b). The Si substrate was etched away after film growth, so that a plate of $\approx 100\mu\text{m}$ diamond with $\approx 1\mu\text{m}$ each of N-doped diamond and SiC was exposed to the x-ray beam. A second sample of Nitrogen-doped CVD grown diamond of similar thickness was used for reference (sample N). The rocking curve of the samples was determined to be $< 0.7^\circ$ (FWHM) wide for sample B and $< 1.3^\circ$ wide for sample N (Fig. 1c) providing a good definition of the momentum transfer in the crystal.

The experiment was performed at the inelastic x-ray scattering station of BL35XU at the SPring-8 synchrotron light source [20]. The energy resolution was set to 6.4 meV by use of the Si(888) reflection in the backscattering monochromator and in the diced spherical analysers with a photon energy $h\nu = 15.82\ \text{keV}$. Detuning of the incident monochromator with respect to the analyser crystals is done by ramping the temperature of the monochromator. Of the 12 analysers available we focussed on the 4 in the scattering plane as providing

information along the common high symmetry direction for longitudinal modes. The energy scale was calibrated for each analyser using the elastic line position and the optical phonon peak from a pure single crystal diamond sample close to the Γ -point at $\vec{Q} = (1.1\ 1.1\ 1.1)$ [8].

Longitudinal spectra were acquired for momentum transfers $\vec{Q} = (00h)$ with $2.06 < h < 3.05$ for the $\Gamma - \text{X}$ line and $\vec{Q} = (hh0)$ with $1.07 < h < 1.53$ for the $\Gamma - \text{L}$ line with a slight offset of some of the momentum points due to the non-collinear scattering vectors for the four analysers. Measurements at the Γ -point itself were not performed due to high background from elastic scattering. For the Brillouin zone boundary point L an additional spectrum at $\vec{Q} = (0.5\ 1.5\ 0.5)$ was acquired where mostly the transverse phonons are observed. All experiments were performed at room temperature and with the sample held in air at ambient pressure.

The use of inelastic x-ray scattering has several advantages over inelastic neutron scattering for the investigation of the phonon dispersions of B-doped diamond. The sample size matches the beam diameter of $\approx 100\mu\text{m}$ very well. The small absorption of the x-rays by the light elements makes the whole cylindrical volume through the sample along the beam available for the experiment. In the case of neutrons the absorption by boron would be quite severe. Large energy transfers as for the optical phonons in diamond are no difficulty in an IXS experiment in contrast to thermal neutrons.

IXS spectra in the energy loss range of the optical phonons are shown in Fig. 2. For the wide range spectrum (Fig. 2e) a background from elastic scattering was subtracted. At the L-point (Fig. 2c and 2e) also the acoustic phonons (LA and TA) are seen. Their peak positions are identical for sample B and N and the peak width is limited by the resolution of 6.4 meV. The LO phonon on the other hand shows a clear peak shift to lower energy in sample B and the peak is slightly broadened. The same observation holds for the LO phonon at the X-point (Fig. 2b), and for the transverse optical TO phonon at the L-point (Fig. 2e) that are shifted and broadened in sample B. Fig. 2a) and 2d) show spectra close to but not exactly at the Γ -point in the two momentum directions at the same distance from Γ . The width of the peak in sample N is still resolution limited, whereas in sample B a severe broadening and a strong shift occur. The indicated peak positions are the centre positions of the peaks determined as the midpoint of the edges at half maximum. The peak positions of sample N match the well known phonon frequencies of pure diamond (164 meV at the Γ -point).

In addition to the expected peaks discussed above, the following observations were made. The elastic intensity at the symmetry forbidden Bragg point (002) and close to (111) became very large both in sample B and N. Along the [001] direction weak intensity of the longitudinal acoustic phonon LA was observed in both samples.

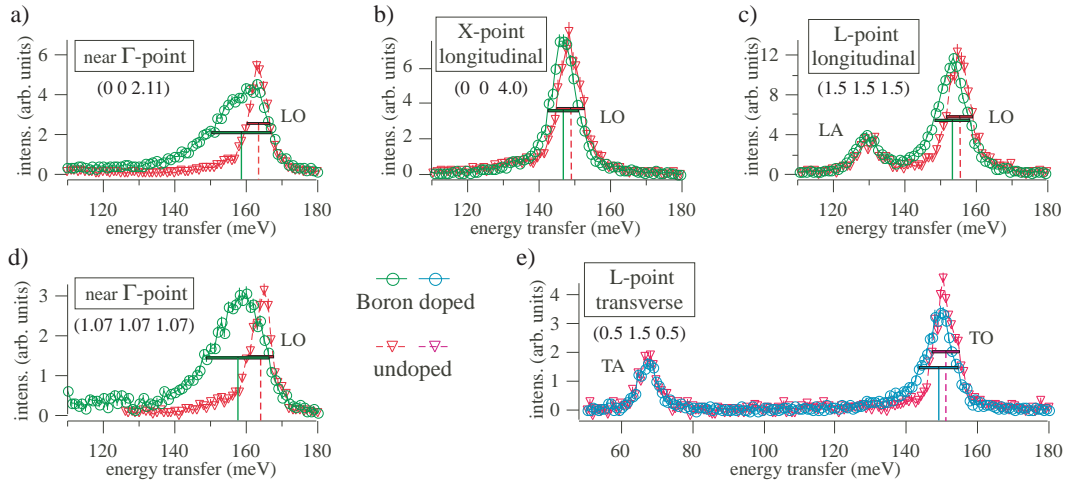


FIG. 2: IXS spectra from sample N (∇) and sample B (\circ) for momentum transfer along the $[001]$ direction (a and b) and the $[111]$ direction (c and d) in a geometry where only longitudinal phonons contribute as well as at $\vec{Q} = (0.5 1.5 0.5)$ where mostly transverse phonons contribute. The total momentum transfer is indicated for each pair of spectra.

Along the $[111]$ direction the LA phonon gives a strong signal and the peak positions for the two samples agree everywhere along this high symmetry line. Along $[001]$ an additional feature becomes visible in the data from B-doped diamond with a dispersion that matches the transverse acoustic phonon TA. This observation and the enhanced intensity at Bragg-forbidden points may be due to disorder in the material [21].

Fig. 3 shows a compilation of all peak positions (a) and widths (c) as determined by midpoint and distance of the two edges of the peaks. The dispersion curve of sample N reproduces the well known results of pure diamond [7, 8]. The middle of the figure (3b) shows the softening-curve i.e. the difference in peak position between samples N and B. The softening is strong close to the zone centre and much reduced at the zone boundary. At the Γ point the strength of softening can be extrapolated as 7 meV. This value is smaller than the almost 20 meV predicted by a VCA calculations [10] and 12.5 meV found in a supercell calculations [14] but it is larger than the apparent peak shift of the single phonon peak in the Raman spectrum of less than 4 meV.

It is tempting to interpret the broadening of the peak widths as a reduction of the lifetime of the phonons. This could be caused by anharmonic effects or by the electron-phonon interaction. Anharmonic effects are predicted to be small even at very high doping [10]. The momentum-dependent lifetime due to electron-phonon interaction is directly related to the electron-phonon coupling parameter λ_q if the density of electronic states at the Fermi level $N(E_F)$ is known. An estimate of $N(E_F)$ can be obtained from ab initio calculations [22]. The lifetime reduction due to electron-phonon coupling should lead to an almost symmetric broadening of the peaks while the peak shape observed in the data is highly asymmetric.

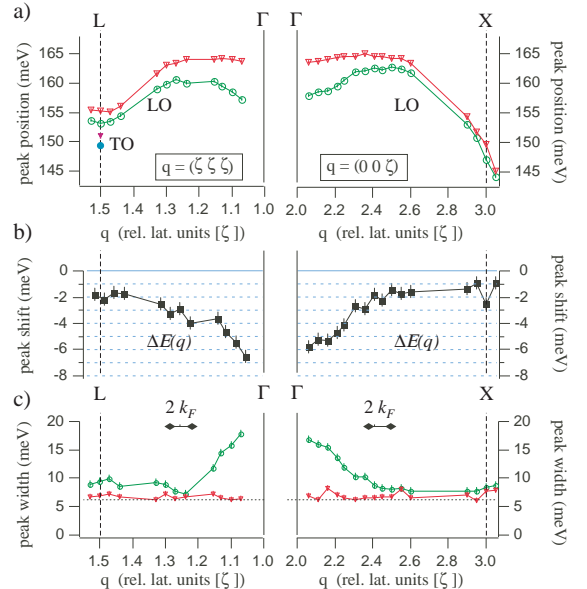


FIG. 3: (a) Dispersion of the optical phonons in sample N (∇) and B (\circ) as determined by the mid-points of the peaks as shown in Fig. 2. In the left part the $\Gamma - L$ and in the right part the $\Gamma - X$ direction is shown. Most data are from the LO phonons but in the left part at the L-point also the TO phonons are indicated. (b) Softening-curve: peak shift for sample B with respect to sample N as a function of momentum. (c) Total peak width FWHM as a function of momentum transfer for the optical phonon peaks. A range of spanning vectors of the Fermi surface as determined from VCA calculations [22] is indicated by a bar.

The electron-phonon coupling parameter λ_Γ determined from the measured peak width at the Γ -point of 17 meV is a factor 2.5 larger than any of the theoretical predictions and we cannot assume that the observed broaden-

ing of the peaks is determined by the electron phonon coupling alone. We must suspect that the broadening of the peaks is much more caused by inhomogeneities of the doping concentration in the sample. The superposition of the more or less strongly shifted peaks leads to the observed asymmetric peak shape. Evidence for a certain inhomogeneity of the doping concentration is also seen in the resistivity curve (Fig. 1b) that shows a rather broad superconducting transition with several steps. The mosaicity and the associated uncertainty of the momentum vector is not responsible for any appreciable broadening of the peaks. The mosaicity should lead to similar effects in sample N that has a wider rocking curve than sample B and no broadening is observed in this case. Also disorder-induced broadening due to the different masses of C and randomly distributed B atoms cannot account for the strong softening [23]. The natural isotope mixture of 80% ^{11}B versus ^{10}B and 99% ^{12}C vs. ^{13}C corresponds to the case of low disorder in Ref. [23], while strong softening due to disorder is expected close to the 1:1 mixture of different but similar masses.

Although no quantitative information can be extracted from the data, the characteristic behaviour of the softening curve gives strong evidence for the coupling mechanism in superconducting diamond. An approximate size scale of the Fermi surface diameter as extracted from the VCA calculation [22] is indicated in Fig. 3. A strong optical phonon softening close to the Γ -point and a much reduced peak shift outside of the volume of the Fermi surface was previously observed in MgB_2 [24, 25]. In diamond a Fermi surface derived from the C sp -electrons would have a rather anisotropic but neckless spheroid shape centred around the Γ -point. In particular the heavy hole band with its large pocket around Γ is a good candidate for a strong electron-phonon coupling [10, 11] since its largest spanning vectors in various directions match the observed softening curve [22].

In conclusion we have measured the phonon dispersions of superconducting B-doped diamond and found a strong shift of the peaks of the optical phonons with respect to N-doped insulating diamond along with a strong broadening. The momentum dependence shows the characteristic behaviour of strong softening close to the zone centre and much reduced softening outside a certain radius inside the Brillouin zone. This shape and the fact that both longitudinal and transverse optical phonons behave the same is consistent with a metallic conductivity in the valence band of diamond and coupling of the phonons to the heavy hole carriers. It thus supports the analogy of B-doped diamond to MgB_2 with the difference that all three optical phonon branches in diamond couple to the heavy hole band and get softened, while in the two dimensional MgB_2 only two modes contribute. Another difference is the intrinsic disorder in diamond due to the doping by impurity atoms. On the other hand the

control of doping by tuning of the B-concentration gives the additional potential of controlling both the electron phonon coupling and the carrier density and thus the superconducting of B-doped diamond.

We would like to thank the Japan Synchrotron Radiation Research Institute (JASRI) for granting beamtime under project numbers 2004B0736-ND3d-np and 2005A0596-ND3d-np. Dr. Sakaguchi at NIMS characterized the samples by secondary ion mass spectroscopy. One of us (MH) would like to thank the Japanese Society for the Promotion of Science (JSPS) for financial support.

-
- [1] E.A. Ekimov *et al.* *Nature* 428 (2004) 542.
 - [2] Y. Takano. *et al.* *Appl. Phys. Lett.* 85 (2004) 2851
 - [3] E. Bustarret, J. Kačmarčík, C. Marcenat, E. Gheeraert, C. Cytermann, J. Marcus, T. Klein, *Phys. Rev. Lett.* 93 (2004) 237005.
 - [4] V.A. Sidorov *et al.* *Phys. Rev. B* 71 (2005) 60502(R).
 - [5] J.-P. Lagrange, A. Deneuville, E. Gheeraert, *Diam. Rel. Mat.* 7 (1998) 1390.
 - [6] H. Umezawa, T. Takenouchi, Y. Takano, K. Kobayashi, M. Nagao, I. Sakaguchi, M. Tachiki, T. Hatano, G. Zhong, M. Tachiki, H. Kawarada, *cond-mat/0503303*
 - [7] J.L. Warren, J.L. Yarnell, G. Dolling, R.A. Cowley, *Phys. Rev.* 158 (1967) 805.
 - [8] J. Kulda *et al.* *Phys. Rev. B* 66 (2002) 241202 and references therein.
 - [9] A.T. Collins, A.W.S. Williams, *J. Phys. C* 4 (1971) 1789.
 - [10] L. Boeri, J. Kortus, O.K. Andersen, *Phys. Rev. Lett.* 93 (2004) 237002.
 - [11] K.-W. Lee, W. E. Pickett, *Phys. Rev. Lett.* 93 (2004) 237003.
 - [12] Y. Ma *et al.* *Phys. Rev. B* 72 (2005) 14306.
 - [13] X. Blase, Ch. Adessi, D. Connetable *Phys. Rev. Lett.* 93 (2004) 237004.
 - [14] H.J. Xiang, Zhenyu Li, Jinlong Yang, J.G. Hou, Qingshi Zhu, *Phys. Rev. B* 70 (2004) 212504.
 - [15] K.-W. Lee, W. E. Pickett, *cond-mat/0509359*.
 - [16] T. Yokoya *et al.* *Nature* 438 (2005) 647.
 - [17] D. Wu *et al.* *cond-mat/0508540*.
 - [18] E. Bustarret, E. Gheeraert, K. Watanabe, *Phys. Stat. Sol. (a)* 199 (2003) 9 and references therein.
 - [19] H. Kawarada *et al.* *J. Appl. Phys.* 81 (1997) 3490.
 - [20] A.Q.R. Baron, Y. Tanaka, S. Goto, K. Takeshita, T. Matsushita, T. Ishikawa, *J. Phys. Chem. Solids* 61 (2000) 461.
 - [21] M. Hoesch *et al.* manuscript in preparation (proceedings of IWSDRM2005, Tsukuba JP Dec. 7-9 2005).
 - [22] We performed the same calculation as in Ref. [11] of VCA using the Wien2k code at a doping level of 2.5 at% and extracted the Fermi surface as well as the density of states at the Fermi level.
 - [23] F. Widulle, J. Serrano, M. Cardona *Phys. Rev. B* 65 (2002) 75206.
 - [24] A. Shukla *et al.* *Phys. Rev. Lett.* 90 (2003) 95506.
 - [25] A.Q.R. Baron *et al.* *Phys. Rev. Lett.* 92 (2004) 197004.